



Article

# Innovative Approaches to Enhance Thermal Efficiency and Reduce Sprue Backflow in Zamak Hot Chamber Injection Moulding

Rita de Cássia Mendonça Sales-Contini<sup>1,2,\*</sup>, André Filipe Varandas Pedrosa<sup>1</sup>, Pedro Leitão<sup>1</sup>, Rafael Resende Lucas<sup>1,3</sup>, Raul Duarte Salgueiral Gomes Campilho<sup>1</sup>, Arnaldo Gomes Pinto<sup>1</sup> and Carlos Roberto Regattieri<sup>1,4</sup>

<sup>1</sup> CIDEM, ISEP, Polytechnic of Porto, Rua Dr. António Bernardino de Almeida, 4249-015 Porto, Portugal

<sup>2</sup> Technological College of São José dos Campos Prof. Jessen Vidal (FATEC), São José dos Campos 12247-014, São Paulo, Brazil

<sup>3</sup> School of Engineering and Sciences, São Paulo State University, Guaratinguetá 12516-410, São Paulo, Brazil

<sup>4</sup> Technological College of Taquaritinga, Centro Paula Souza, Taquaritinga 15900-000, São Paulo, Brazil

\* Correspondence: [remsc@isep.ipp.pt](mailto:remsc@isep.ipp.pt); Tel.: +351-22-83-40-500

**How To Cite:** Sales-Contini, R.d.C.M.; Pedrosa, A.F.V.; Leitão, P.; et al. Innovative Approaches to Enhance Thermal Efficiency and Reduce Sprue Backflow in Zamak Hot Chamber Injection Moulding. *Journal of Mechanical Engineering and Manufacturing* 2025, 1(1), 4. <https://doi.org/10.53941/jmem.2025.100004>.

Received: 5 May 2025

Revised: 20 May 2025

Accepted: 28 May 2025

Published: 3 June 2025

**Abstract:** This study uses a Design Science Research (DSR) approach to improve the thermal performance of an injection nozzle for die-casting Zamak components. This involves identifying the problem, creating an iterative design and simulation, implementing solutions and evaluating them through computational and experimental validation. A combination of computational fluid dynamics (CFD) simulations and thermal modelling in SolidWorks Flow Simulation was used to analyse temperature distributions and identify geometric modifications aimed at reducing heat loss and preventing solidification within the nozzle. Key results include the development of a modified nozzle design featuring reduced length and optimised channel diameters, which has led to improved thermal efficiency. Experimental validation using temperature measurements near the nozzle tip demonstrated close agreement with simulation predictions, confirming the efficacy of the optimised design. The findings conclude that strategic geometric alterations and refined modelling assumptions can significantly improve heat retention, ensuring more reliable Zamak injection processes.

**Keywords:** sprue backflow; thermal management; die-casting; nozzle design innovation; process automation; Zamak moulding; injection system reliability

## 1. Introduction

In today's industrial sector, it is possible to confirm that the automotive industry is at the forefront of innovation and efficiency, mostly due to the competition felt in this sector. Nowadays, since the automobile is engraved in the day-to-day lives of the world's population, it is expected that this industry will represent a large business volume [1]. Not only that, but to build a vehicle now, there are a lot of manufacturing processes involved, from textiles to plastic and metal forming. Therefore, there is a large proportion of the metalworking industry that is only focused on manufacturing vehicle components [2].

The automotive industry is one of the most competitive sectors globally, driving a continuous demand for innovation to produce faster, cheaper products without sacrificing quality. Manufacturers must focus on three key pillars: competitiveness, quality, and flexibility [3,4]. Competitiveness is influenced by five factors: new market entrants, innovative products, customer bargaining power, supplier influence, and industry rivalry [5,6]. Quality



**Copyright:** © 2025 by the authors. This is an open access article under the terms and conditions of the Creative Commons Attribution (CC BY) license (<https://creativecommons.org/licenses/by/4.0/>).

**Publisher's Note:** Scilight stays neutral with regard to jurisdictional claims in published maps and institutional affiliations.

is pressured by customer expectations and international safety and environmental regulations [7,8]. Flexibility in production is crucial for sales volume as it enables manufacturers to tailor products to customer needs, though they must balance this with the potential for decreased productivity and increased costs due to product variety [9,10].

Metal injection moulding at high pressure is one of the most widely used processes for manufacturing components with complex geometries and moderate mechanical strength requirements [11]. However, injecting small components made of light alloys, such as Zamak, can present challenges that are sometimes difficult to overcome. Zamak is a metal alloy consisting mainly of zinc, with the addition of aluminium, magnesium and copper. Its typical proportions are approximately 90% zinc, 4% aluminium, 0.5% magnesium and 1% copper. This alloy is valued for its excellent mechanical properties and casting capacity, which allow complex and detailed parts to be produced through die-casting with good dimensional stability and surface finish. Despite its limited heat resistance and susceptibility to corrosion in aggressive environments, Zamak is widely used in the automotive industry and beyond to manufacture components requiring mechanical strength and aesthetic quality, such as door handles, locks and engine casings [12].

In mechanisms that require mechanical control, such as those using Bowden cables, ensuring efficient connections for motion transmission is essential. Bowden cables are highly versatile for transmitting motion, allowing for various assembly configurations, including non-linear layouts, without reducing efficiency [13–15]. In the automotive industry, these cables have a wide range of applications, including door and bonnet locks and brake and clutch actuation systems [16]. Terminals are commonly manufactured by hot chamber casting, a process in which molten metal is forced into a mould and, upon cooling, forms the final part. Advantages of this manufacturing method include high geometric accuracy, tight tolerances, high productivity and consistency, a good surface finish, and the ability to produce thin walls [17,18].

On the other hand, it is challenging to produce big parts because this process tends to retain gases in the moulded figure, giving rise to defects. The other drawback is that the hot chamber die-casting only allows casting metal alloys with low melting points, such as Pb and Zn-alloys, such as Zamak, which is the most commonly used to produce the terminals for the Bowden cables [19]. This temperature constraint is due to most of the components used in these machines being made from steel alloys; therefore, the material used to cast must have a lower melting point than the components in contact with the molten metal [20]. Over the years, there have been several scientific studies on the production of Zamak terminals using the hot chamber die-casting method. Pereira et al. [21] developed a study regarding the premature breakage of the sprue. Besides solving the initial problem, the author reduced the sprue size by 62.6% and the gas entrapment by 10.2%. Another study made on this subject was presented by Pinto et al. [22] to improve the efficiency of the Bowden cable injection process. In this work, a finite element tool was utilised, and the authors came to the following conclusion: the injection pressure and speed cannot be too high to avoid the turbulent flow of the molten metal, and the cooling time has to be long enough to allow the metal to solidify. It was also analysed the impact of the number of injection points and it was verified that one injection point is better. Similar conclusions have been drawn by Silva et al. [23] regarding the hot chamber die-casting of aesthetic components in a study that intended to mitigate successive problems detected on the surface of these kinds of components. The previous study of Pinto et al. [22] was also extended later to the moulds' improvement regarding the same type of product: Bowden cable Zamak terminals [24]. Other studies have also been focused on Bowden cables, but not directly related to the metal injection process, such as the study presented by Vieira et al. [16], which used a different concept of movement, allowed the fabrication of Bowden cables with increased length without quality problems. Also using automation, Moreira et al. [9] developed a piece of integrated equipment able to deal with various production operations previously performed in an isolated way, increasing the productivity of this product and saving logistics operations. This concept was also later improved by Sousa et al. [25], improving the quality and productivity of Bowden cables' production. Recently, Olbrich and Lackinger [26] have drawn a state of the art regarding the production of Wire harness for the automotive industry.

Despite the advanced state of the automotive industry and the implementation of various manufacturing technologies, there are still challenges in improving the Zamak hot chamber injection moulding process, particularly in mitigating sprue reflow, which reduces production efficiency. Current solutions lack a comprehensive understanding of, and systematic approach to, addressing the process's inherent thermal and flow inefficiencies. This study aims to address this issue by investigating novel modifications to the injection system, such as adjustments to the intake angle, nozzle design and thermal management, using the Design Science Research methodology. This work's scientific contribution lies in developing an integrated framework combining empirical testing, thermal simulations, and practical implementation to improve process reliability and production efficiency, thus advancing knowledge in die casting improvement.

## 2. Methodology

To pursue the main goal of this work, the Design Science Research (DSR) methodology has been adopted, dividing this work into six stages: (a) Problem identification, (b) goal setting, (c) design and development, (d) implementation of the solution, (e) evaluation of the solution and (f) conclusions. The DSR methodology has gained a growing number of followers and seen new developments in the last decade, as it is perfectly suited to improving existing systems that need to be redesigned for better performance, as well as new products based on existing ones, such as information systems [27,28] and automatic liquid filling systems [29]. According to Teixeira et al. [30], the DSR methodology is particularly useful because it is mainly aimed at solving technical and technological problems, is based on very solid principles, is flexible to adjust to different situations, and allows complex and sometimes ill-defined problems to be overcome. Based on the work of Devitt and Robbins [31], Siedhoff [32] introduced design thinking in the phases initially defined for the DSR methodology, adapting the methodology to continuous improvement problems. In any case, the methodology can also integrate research stages [27], always based on an initial diagnosis phase with clear identification of the problem, development of solutions and prescriptive research, allowing the extraction of solutions that could be used to solve problems and making the best decisions for future identical situations [33]. This methodology was successfully used by Eiras et al. [14] to increase the flexibility and productivity of equipment capable of producing the first subset that constitutes the product commonly known as the Bowden cable. Tojal et al. [34] used this methodology to implement this new injection subset in the die casting process, achieving beneficial results such as reduced consumption, procurement costs and waste, as well as reduced operation numbers and increased equipment availability. Zhou et al. [35] solved similar problems by optimising the selection of modification settings, modifying universal machine tool settings and compensating for machine geometric errors.

This methodology was adapted to the present work, and it was possible to define six stages: (a) Problem identification (diagnosis), (b) brainstorming and possible solutions to implement, (c) development, (d) critical analysis of the adopted approach, (e) implementation, and at last (f) analyses of the results and possible theorizing. From these seven stages, three concepts were tested for their feasibility: (1) Intake angle adjustment, (2) Injection machine parameters, and (3) Alternative material family and coatings. Problem diagnosis was of utmost necessity to do a deep dive analysis of the die-casting injection system composed of three main components: injection pump, injection nozzle Figure 1.

The moulding process comprises four components: the frame and the upper and lower moulds (see Figure 2). The mould shapes the Zamk terminal, while the frame couples and cools the mould. This frame-mould system enables the injection reference to be changed quickly without adjusting the contact between the nozzle and the frame. While the upper and lower frames remain assembled on the machine, the mould assembled on the frame is changed as necessary. The mould cooling system allows water to pass through channels designed for this purpose and positioned for optimal cooling. The operating temperature of the frame is around 40 °C. However, this temperature can vary due to obstructions in the channels and changes in the temperature of the water supply.



**Figure 1.** (a) Injection nozzle assembled in the hot-chamber die-casting machine, and (b) nozzle with the electrical resistance assembled on its tip.

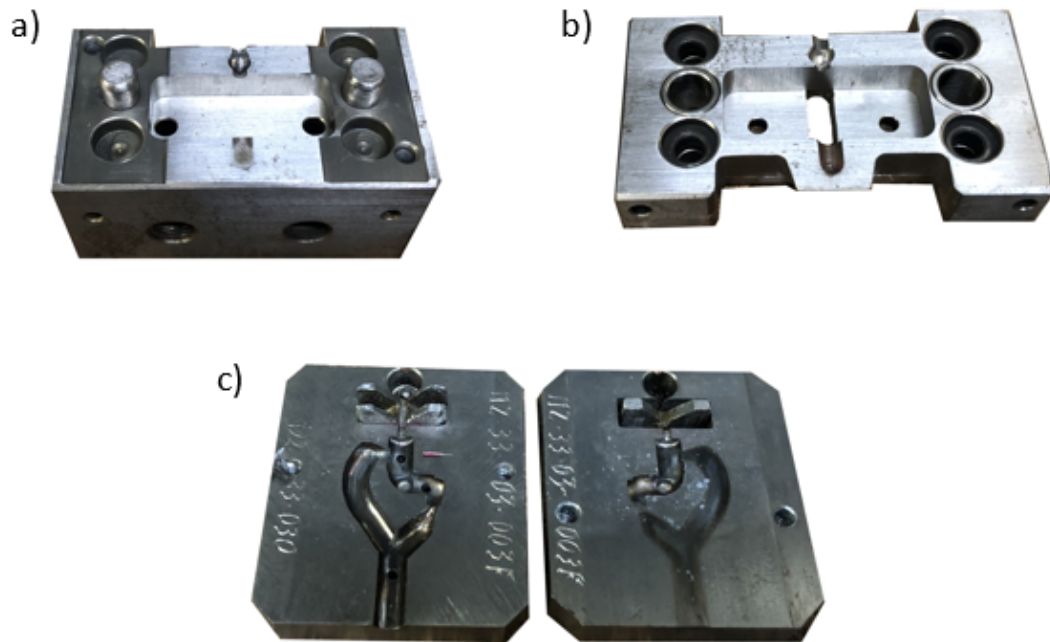


**Figure 2.** (a) Upper frame for coupling and cooling the mould; (b) Lower frame for coupling and cooling the mould; (c) Moulds for forming the terminal in ZAMAK alloy used in the hot-chamber die-casting machine.

During this analysis, it was found that the stoppages in production were due to failed injections caused by a blockage of solid Zamak in the injection nozzle. Every time this happened, the machine was stopped between 30 to 60 min, significantly reducing production efficiency. It was possible to realise that this problem was due to a temperature drop in the tip of the injection nozzle paired with the geometric configuration of the injection channel, which is at a  $45^\circ$  angle, causing a counter exit if the metal solidifies, as it can be seen in Figure 3. If the solid metal in the injection nozzle cannot be extracted, it breaks and originates the blockage previously mentioned. To balance this phenomenon, the maintenance team tends to increase the temperature of the heating electrical resistance around the nozzle (Figure 1b), but this has a negative impact because the temperature increase reduces the lifespan of the injection system components. With the problem identified, the next step was to think about different solutions to overcome the problem.

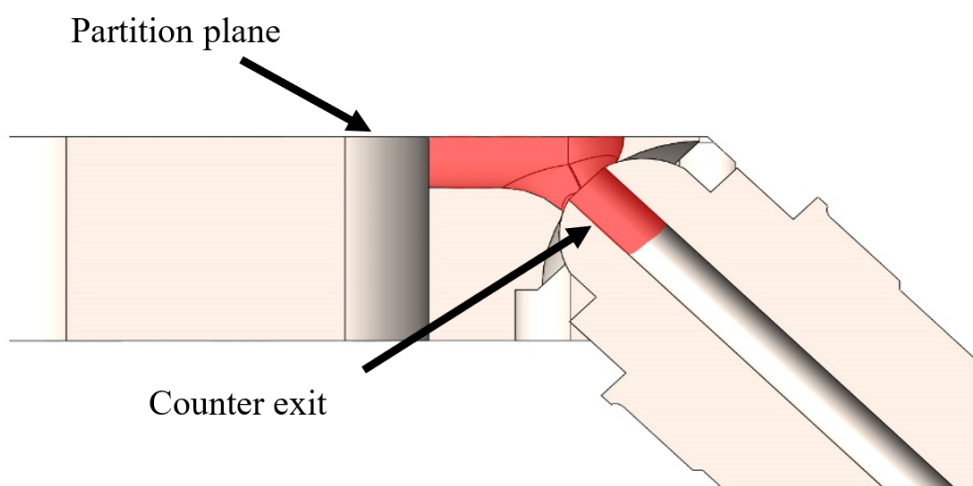


**Figure 3.** Lower structure-nozzle assembly with the problematic area of the gate marked in red.

Starting the brainstorming phase, the first approach was to change the injection channel's angle since the problem lies in the counter exit caused by the  $45^\circ$  admission angle. Thus, there were two possibilities to change the admission angle from  $45^\circ$  to  $90^\circ$  concerning the partition plane. The first one was to develop a new pump. This idea was quickly discarded due to the volume of modifications needed in the machine, representing an investment

high enough to demotivate the management team, and this solution was not appropriate to the current industrial setting. The second approach was to try maintaining the current pump but changing the injection nozzle so that the admission of the molten metal in the mould was made from a 90° angle, Figure 4.

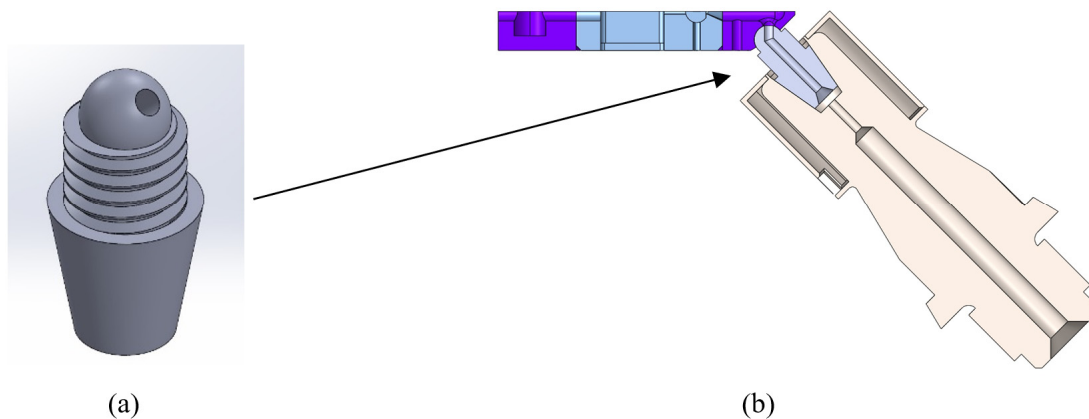


**Figure 4.** (a) New design of the nozzle, and (b) nozzle assembled into the hot-chamber die-casting machine.

In the development phase, a few changes had to be made to the current setup to make the solution plausible: the threaded connection was replaced by a conical connection to ensure the correct placement of the injection channel, and the touching point of the injection nozzle in the mould also needed to be adapted. Thinking that this concept was promising, a prototype was produced. The first problem observed with this concept was in the tuning stages of the assembly, although it was hard to properly align the injection channel of both components properly. Thus, a test was performed replicating the conditions experienced on the industrial floor and following the set of parameters: Injection pressure 5 bar, Filling and Cooling time of 0.35 s and 0.10 s, respectively, nozzle heating temperature of 600 °C (873.15 K) and Zamak temperature of 430 °C (703.15 K). During these preliminary tests, it was noticed that this concept had some problems that became unreliable and unusable because of that. From the outset, it was noted that the nozzle could not maintain the necessary temperature, so the Zamak did not solidify into it. Moreover, the part cannot be extracted from the mould, and the conic connection did not create a tight connection, allowing the molten Zamak to escape after 40 injections. In Figure 5, it is possible to observe the leakage of Zamak in the contact between the nozzle and the tip of the nozzle holder. Tightness problems were observed in all nozzles, regardless of the material used in the nozzle (AISI 316 and AISI H13 quenched and nitrided). This analysis, as well as others presented below, correspond to the critical analysis of the results, which is an iterative phase with the brainstorming phase.

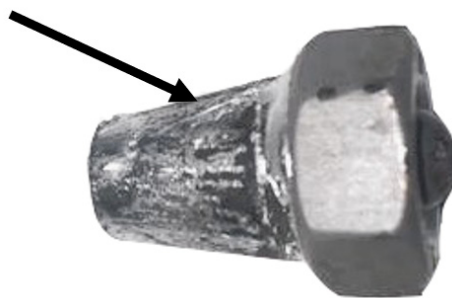


**Figure 5.** The aspect of the degraded AISI 316 nozzle after preliminary tests and after Zamak leakage.

The AISI 316 nozzle withstood more injections without the Zamak passing through. This phenomenon is because stainless steel has a lower hardness than AISI H13 steel quenched and nitrided, so the conical surface of the nozzle conforms to the conical surface of the tip due to the pressure of the nozzle touching the structure. However, this factor was not enough to overcome the cast Zamak's injection pressure and high fluidity. Due to the lower hardness of AISI 316 during the machine tuning process, the nozzles tested in this material suffered plastic deformation, putting their proper functioning at risk. For the reasons pointed out, this concept was discarded. Considering the lessons learned in the preliminary studies carried out and being familiar with the process, the next step was to improve the intended system, the flush nozzle concept.

To reduce the cost of prototyping, Solidworks® was used to build a model of the injection system, from which it would be possible to carry out several simulations. This includes all components around the most critical zone, i.e., the nozzle and the contact area between the nozzle and the structure. This model came with its challenges; the threaded connection had to be removed, and the thermal conductivity of the components was kept the same during the simulation, even though it changed with the temperature.

Another simplification was implemented in the heating band; the heating power of the resistance is higher in the middle and lower in the extremities, but, to simplify, and due to the lack of information to quantify this difference, it was assumed that the power is uniform throughout the length of the heating band. An adaptation was also made to the tip to simulate the part of it that is submerged in liquid Zamak. The tip was divided into two parts, and the lower part was assigned a temperature of 430 °C (703.15 K), equalling the temperature of the Zamak in the crucible. Due to some limitations of the software, the threaded connections between the nozzle and the tip were removed, and it was assumed that contact was only made by two cylindrical surfaces. The thermal conductivity of materials varies with increasing temperature. However, in the model, a constant value was used for each of the materials.

The last simplification was the resistance that assumed a constant value, knowing that its power is not constant along its entire length. The thermal model developed in Solidworks® v. 2022 Flow Simulation allows simulating of thermal transference by conduction, convection and radiation. This allowed to test different possibilities and see the impact of different changes in geometry and materials, reducing the cost associated with manufacturing prototypes. To simplify the model and make the simulation times significantly lower, only the components that have a direct influence were modelled; these were the injection nozzle, the mould, and the heating band Figure 6.

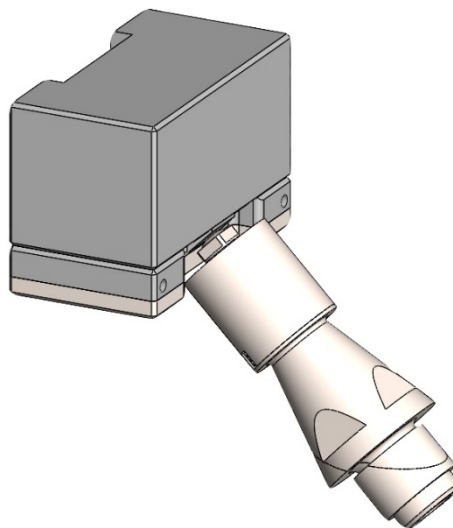


**Figure 6.** Solidworks® modelling of the nozzle and corresponding contact with the mould.

All boundary conditions must be defined to carry out the simulations. Table 1 defines the physical conditions assumed for each of the elements of the injection system: material, thermal conductivity, and temperature. Tables 2 and 3 contain all the parameters of the mesh definitions (cuboid type) to set the SolidWorks® software v. 2022 for modelling the nozzle. In Figure 7, it is possible to observe the mesh generated with these same definitions.

**Table 1.** Physical conditions parameters used for each of the elements of the injection system.

Components	Material	Thermal Conductivity [W/m·K]	Temperature [K]
Nozzle	AISI H13	29	-
Top tip	AISI H13	29	-
Down tip	AISI H13	29	703.15
Electrical resistance	AISI316	15	873.15
Glass	AISI 316	15	-
Frame	AISI D2	23	353.15
Lower frame	AISI D2	23	-
Upper frame	AISI D2	23	-

Mould	AISI D2	23	-
-------	---------	----	---

**Table 2.** Input Parameters used in the SolidWorks® software to global mesh settings for modelling the nozzle.

Type	Automatic
Level of initial mesh	7
Ratio factor	3.5
Advanced channel refinement	Selected

**Table 3.** Input Parameters used in the SolidWorks® software to local mesh settings for modelling the nozzle.

	Refining Cells	Channels	Advanced Refinement
Level of refining fluid cells	2		
Level of refining solid cells	3		
Level of refining at fluid/solid boundary	3		
Characteristic numbers of cells across channel		20	
Maximum channel refinement level		2	
Small solid feature refinement level			2
Curvature level			2
Tolerance level			2

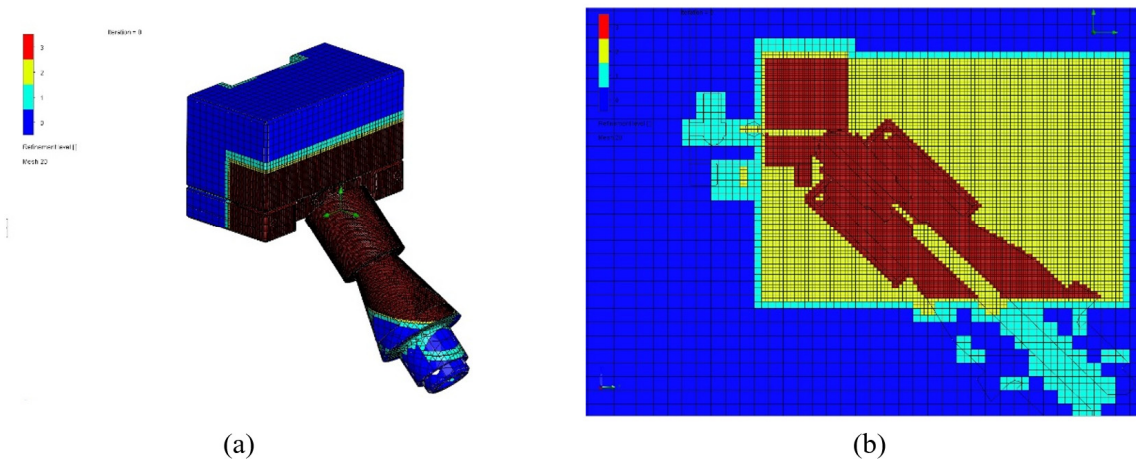


**Figure 7.** (a) 3D mesh visualisation in solids; (b) Mesh sectional view.

After verifying that the mesh had a satisfactory refinement in the critical areas, we moved on to defining the thermal contact resistances between the various elements of the injection system. The values used for contacting thermal resistance were based on scientific articles published on this topic—heat transfer. Assuming that contact thermal conduction values for AISI H13 steel vary between 0.75 kW/m<sup>2</sup>K and 9 kW/m<sup>2</sup>K depending on contact pressure, roughness and temperature [36,37], contact thermal conduction values within that range were selected, adapting to the conditions observed in the machine. Contacts with lower pressures correspond to a higher contact thermal resistance, while if the contact pressure between two components is higher, the contact thermal resistance will be lower. Using this principle, a contact thermal conduction between the nozzle and the tip of 4 kW/m<sup>2</sup>K was assumed, and 1.1 kW/m<sup>2</sup>K for the remaining components, as they are in contact but do not suffer significant pressure. Knowing that contact thermal resistance is the inverse of contact thermal conduction, it leads to the following values: 0.00025 m<sup>2</sup>K/W and 0.0009 m<sup>2</sup>K/W, respectively.

Finally, the objectives of the simulation were defined, i.e., the goals to which this calculation method converges. The following goals were selected: Average Temperature (Fluid) 1; Average Total Temperature 2; Average Heat Transfer coefficient 4; Average Heat Flux 5; Average Temperature (Solid) 11. The most relevant for the objective of this work is the Average Temperature (Solid), which indicates the temperature of the solids at a given point. In these simulations, the focus was on the geometric component of the constituents of the injection system, in order to obtain the most favorable geometric combination. The objective is to have a higher temperature along the length of the nozzle injection channel, eliminating the risk of injection failures due to the solidification of the Zamak in the channel. Once the model was defined, an iterative process was followed with the aim of

improving the system in order to retain a greater amount of heat. The materials utilised were the same currently being used in the die-casting machines and previously pointed out in Table 1. Particular attention was paid to the nozzle close to the contact zone being this area the main focus of the analysis of the temperature evolution. Thus, twelve points were considered in the simulations to collect data about the temperature along the injection nozzle, as shown in Figure 8.

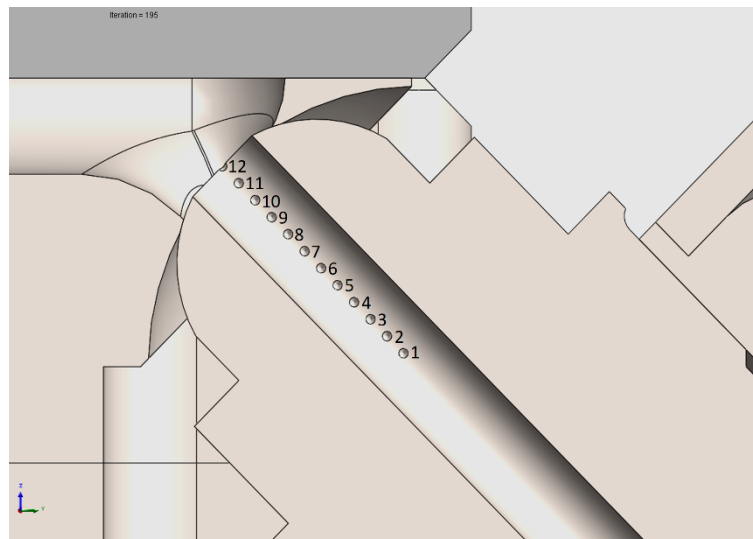


**Figure 8.** A set of points used to measure the temperature.

With the model completely defined, successive simulations were performed using the configuration utilised in the industrial setting. An empirical iterative strategy was thus adopted to identify the problem preventing the desired results from being achieved, find a solution to implement, analyse the results again, and identify points for improvement that would consistently bring the results closer to the desired values. After the first iteration, three more iterations were carried out, whose values are described in the results, and whose main actions were to improve a selection of the geometry and contact zone that best corresponded to the properties of the selected materials. The results of the first simulation were used as a control. After analysing the first set of results, changes were thought out and implemented in the design of the nozzle to reduce the heat lost to the exterior of the injection nozzle material, reducing the heat exchange by convection to the exterior. Hence, material was added to the end of the nozzle (Figure 9), causing heat to be retained in the nozzle, reducing convective losses to the outside.

It is important to note that the geometric limitations of the injection system always condition changes to the injection nozzle. This was the only change made concerning the previous simulation.

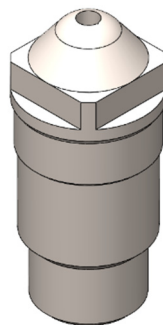


**Figure 9.** Configuration of the nozzle design for the second simulation into the empirical iterative process of improvement.

In the second simulation, it was observed that the cold structure, when compared to the nozzle, involved its end. Thus, this area was removed, and the contact geometry was improved. The nozzle used in the previous simulation was maintained, and just the contact zone was changed, as shown in Figure 10. The third iteration/simulation was performed based on this configuration.

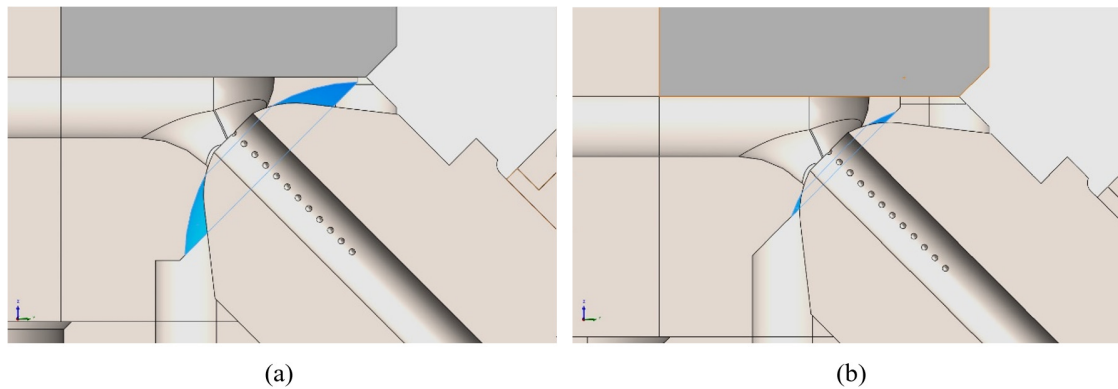


**Figure 10.** Graphical comparative study of the contact area between the nozzle and the mould structure: (a) second simulation; (b) improvement performed for the third simulation.

Given that the results still did not meet expectations, the reasons for the ineffectiveness of the solution used in the previous iterations were studied, to introduce new improvements. It must be assumed that the heat source is the resistance, and that this heat will disperse, particularly towards the end of the nozzle. By reducing the nozzle length, conduction heat losses will be lower, which in theory causes an increase in temperature at the end of the nozzle, eliminating the solidification of Zamak inside. Therefore, in the 4th simulation, the length of the nozzle was reduced as much as possible, keeping as much material as possible, as this is beneficial, as proven in the 2nd simulation. It was necessary to add material to the abutment area of the structure to meet the initially imposed requirement and compensate for the length removed from the nozzle. These changes are illustrated in Figure 11.

To verify that the diameter of the injection channel currently used was, in fact ideal in terms of thermal efficiency, 1.8 mm, a simulation was carried out in which the diameter of the channel was reduced to 1.5 mm, and another under the same conditions, however with an injection channel diameter of 1.9 mm. The maximum diameter of the channel is restricted by the diameter of the hole through which Zamak enters the stirring system, approximately 2.5 mm. It is important to ensure that there is some margin between the two diameters to allow the hot chamber die-casting machine to be adjusted.

Taking the 4th simulation as promising, the nozzle and structure of this new concept were manufactured, and a machine was chosen to apply them and validate the results obtained by simulation. This phase corresponds to the implementation.

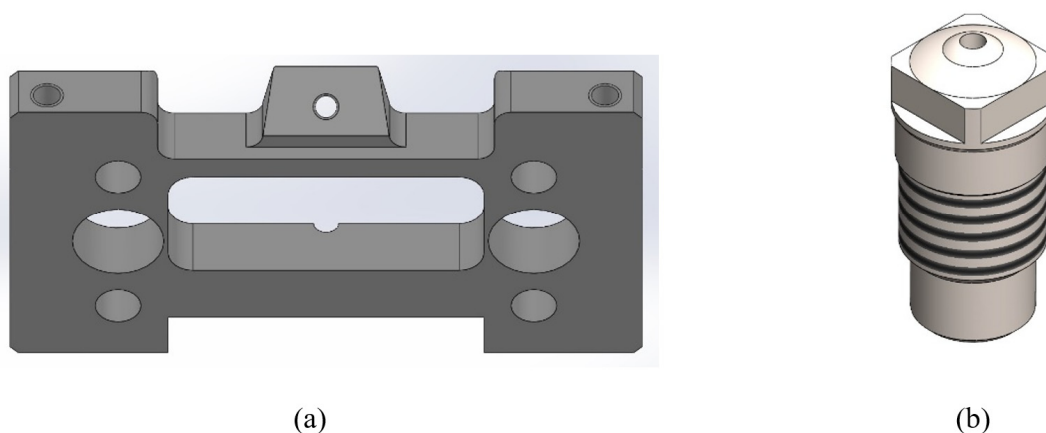


**Figure 11.** Changes performed from the 3rd to the 4th iterations: (a) changes performed in the mould structure; (b) changes performed in the nozzle.

### 3. Results

The simulations explored various factors, including contact geometry, nozzle length and diameter, and heat retention strategies, to approach the optimal design systematically. Initial simulations, for example, identified shortcomings in heat retention and solidification risk, prompting modifications such as reducing the nozzle length and adjusting the contact areas. Four different Computational Fluid Dynamics (CFD) simulations were conducted to study the Zamak's flow inside the nozzle, namely by assessing the temperature gradient in twelve different

points, which incorporated these refinements, was the most promising and was validated through subsequent manufacturing and testing. These four simulations were performed iteratively to analyse and improve the thermal and geometric performance of the nozzle in the Zamak injection system. Specifically, they were used to evaluate temperature distribution, assess the effects of geometric modifications and identify the configuration that best prevents Zamak solidification during injection. This iterative process was essential because each simulation provided insights that informed subsequent design adjustments, leading to a more effective and efficient nozzle configuration [38].

As can be seen in Figure 8, twelve indentations were made inside the injection channel at intervals of 0.5 mm, starting from the injection nozzle's tip, to enable measurement and comparison of temperatures along the injection nozzle in various simulations, resulting in a length of 5.5 mm. Table 4 presents the results obtained for all four simulation rounds.

**Table 4.** Temperature measurements, in Kelvin degrees, from the four simulations.

Distance to the Outlet (mm)	Set-Point	1st Simulation T(K)	2nd Simulation T(K)	3rd Simulation T(K)	4th Simulation T(K)	Average $\pm$ Standard Deviation
5.5	1	760.29	758.52	761.70	799.12	769.91 $\pm$ 16.90
5.0	2	752.65	751.90	755.27	794.75	763.64 $\pm$ 18.00
4.5	3	743.83	744.60	748.19	789.94	756.64 $\pm$ 19.30
4.0	4	733.64	736.52	740.33	784.62	748.78 $\pm$ 20.83
3.5	5	721.77	727.34	731.38	778.70	739.80 $\pm$ 22.72
3.0	6	708.12	716.66	720.94	771.88	729.40 $\pm$ 24.96
2.5	7	692.83	704.08	708.59	763.71	717.30 $\pm$ 27.40
2.0	8	675.66	688.84	693.56	753.37	702.86 $\pm$ 29.89
1.5	9	655.85	669.93	674.80	739.31	684.97 $\pm$ 32.13
1.0	10	632.09	645.97	650.90	719.27	662.06 $\pm$ 33.74
0.5	11	605.34	618.26	623.13	692.69	634.86 $\pm$ 34.02
0.0	12	593.07	605.46	610.27	681.52	622.58 $\pm$ 34.60

Figure 12 depicts the discretised temperature gradient for the four simulations carried out, plus the indication of the Zamak's melting point, showing immediately that the fourth simulation is the most promising to adopt since it enables more liquid Zamak to flow through the final stages of the nozzle.

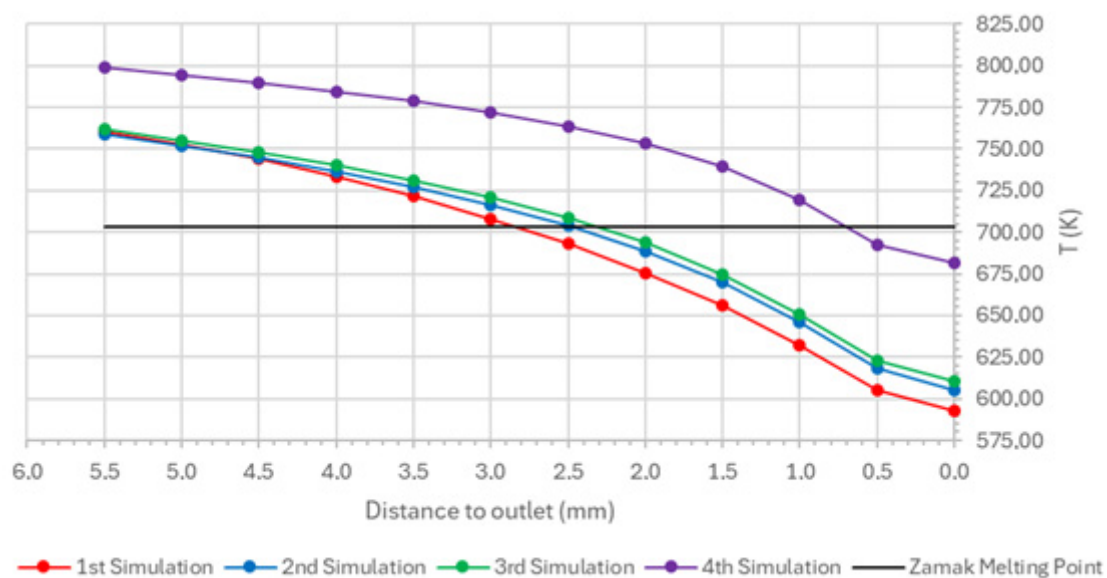


**Figure 12.** Illustration of the temperature evolution along the nozzle for the four simulations.

After assembly, parameter adjustments were made. One focus was reducing the resistance temperature to increase component lifespan. With lower temperatures, the heat treatment of quenching and tempering and the nitrided layer exhibit a longer lifespan until they lose properties. Various temperatures were tested to understand the thermal limit of this concept. It was agreed upon that at 560 °C (833.15 K), the resistance temperature, the machine operated correctly without injection failures. The newer parameters are indicated in Table 5.

**Table 5.** Newer machine parameters set.

Injection pressure	5 bar
Cooling time	0.10 s
Filling time	0.35 s
Heating band temperature	600 °C/873.15K
Zamak Temperature	430 °C/703.15K

The possibility of conducting a thermographic analysis to perceive temperature distribution in the Zamak injection system was studied to validate the theoretical model and compare it with the results obtained from the theoretical model simulation. However, due to the high cost associated with outsourcing this service to an external entity, the organisation deemed it did not bring added value, justifying the investment. This decision was made as the newly implemented concept fulfilled all previously established requirements and was functioning correctly. Therefore, to validate the theoretical model without affecting production, a type K probe with an accuracy of approximately  $\pm 1.5$  °C or  $\pm 0.4\%$  of the reading was used to measure the temperature at the nozzle's tip. Attempts were made to measure the temperature approximately 1 mm from the nozzle's tip. Table 6 presents the obtained results.

**Table 6.** Comparison of actual temperatures with simulation results.

	Heating Band Temperature (°C/K)	Temperature Point—1 mm from the Tip of the Nozzle (°C/K)	Difference (°C/K)
4th Simulation	600.00/873.15	446,12/719.27	153.88
Case study	560.00/833.15	390.00/663.15	170.00

#### 4. Discussion

The impact of geometric modifications on thermal performance is one of the key findings of this case study. It was identified that reducing the nozzle length and optimising the contact geometry significantly improved heat retention. This is particularly important as it minimises heat loss through convection, which was a major issue in previous designs. The modifications led to a more efficient nozzle configuration, which was validated through experimental testing that showed close agreement with simulation predictions [39].

The contour condition established that maintaining a resistance temperature of 560 °C (833.15 K) was critical for the proper functioning of the injection system without failures. This finding aligns with Chen [40], who emphasised the importance of temperature control in injection moulding processes. The adjustments made to the nozzle design not only improved thermal efficiency but also extended the lifespan of the components involved, as lower operational temperatures reduced the risk of material degradation. Analysing the previously presented results, it is evident that the simulation exhibits fewer losses than reality. The temperature difference between the resistance and the point 1 mm from the nozzle's tip is only 153.88 °C (K) in the simulation, whereas a difference of 170 °C (K) was observed in the machine. Based on these data, it was concluded that the simulation has a relative error of 9.48%. This error is mainly attributed to the simplifications made in the theoretical model to facilitate its execution.

It is also recognised that despite efforts to measure the temperature at 1 mm from the nozzle's tip as accurately as possible, exact precision in this measurement cannot be guaranteed. Other factors negatively influencing the injection machine include cycle time, air or water leaks in the mould area, and mechanical wear on injection components. When compared to Saifullah et al. [41] the findings highlight a more systematic approach to addressing thermal inefficiencies. In their studies, Saifullah et al. [41] focused on singular aspects of the injection process, such as material properties or isolated design features. In contrast, this study's comprehensive approach, which integrates CFD simulations with empirical validation, provides a more holistic understanding of the factors influencing thermal performance in Zamak injection moulding. This advancement is significant as it offers a framework that can be applied to other materials and processes within the industry.

Despite these factors, it can be asserted that the theoretical model fulfilled its purpose, as it reflected reality as closely as possible and led to the development of a highly beneficial concept for the organisation. During the period covered from 2nd and 3rd month of the year, the machine was stopped for approximately 20 h due to injection system issues, resulting in a machine availability loss of 5.2%, thereby hampering production and human resource utilisation. During this period, eight nozzles and six resistances were used, resulting in expenditures of €128 on nozzles and €408 on resistances. While these amounts may not appear significant individually, it is essential to emphasise that the company owns approximately 60 machines. Multiplying the aforementioned values

by 60, they represent approximately €32,160 over eight months, focusing solely on these two components, equating to €4,020 monthly expenditure on nozzles and resistances.

Considering that the nozzle was installed in the 5th month of the year, it is evident that the machine was only stopped for injection system issues for 2.5 h, caused by the failure of the resistance reused from the previous concept. This resulted in a mere 0.71% machine availability loss, translating to a 4.49% availability gain. These values are auspicious, as the nozzle has operated for two months without any injection failure issues, double the average lifespan of nozzles used in the previous concept. However, due to its limited operating time and the unknown lifespan of this new concept, quantifying the economic gain in terms of reduced wear component consumption is challenging. This shorter nozzle concept reduces unplanned intervention time, increases equipment availability, and reduces wear component consumption, namely the nozzle and resistance. Consequently, the machine's OEE has been significantly improved. This phase closes the DSR methodology applied, through the results analysis and theorizing. It can be stated that shorter nozzles with the lowest contact area with the mould bottom frame lead to an increased temperature of the nozzle channel (less temperature lost), avoiding the need of increase the energy provided by the electrical resistance, which would be translated in shorter nozzle lifespan, due to the abrupt drop in hardness under the range of temperatures needed to keep the molten Zamak in liquid state into the nozzle channel. This approach not only enhances the machine's overall efficiency but also contributes to sustainable practices by minimizing energy consumption and extending the lifespan of critical components.

## 5. Conclusions

The study thoroughly examined various aspects of the automotive industry, equipment design, and casting of components. It identified challenges and potential solutions, highlighting the importance of iterative design processes and technological advancements. Despite some hurdles, implementing new concepts showed promise, particularly in addressing thermal inefficiency issues. Overall, the research successfully tackled the initial problem and met its objectives, with a notable increase in equipment availability:

- Three main themes were introduced: the automotive industry, equipment design, and casting, with a focus on the economic impacts of AI and the components industry;
- Equipment design, an iterative process crucial for product success, requires consideration of various materials and manufacturing processes aided by tools like Ashby diagrams and PRIMA matrices;
- Advancements in technology, particularly computer-aided design programs, have significantly reduced prototype development costs through 3D modelling and simulations;
- Injection casting, distinguished between hot-chamber and cold-chamber methods, was explored alongside the influence of zinc alloying elements on the produced parts;
- Preliminary studies revealed that many approaches to the problem were not viable due to process or company constraints;
- Implementing a new pump concept to change the intake angle proved costly and inconclusive, but a different nozzle concept showed promise despite issues;
- Investigation of Zamak machine injection parameters yielded inconclusive results due to external factors;
- The hypothesis of manufacturing injection system elements in other materials, such as ceramics or HVOF coatings, faced challenges such as fragility and oxide layer formation;
- A theoretical model was developed to improve heat conduction to the injection nozzle's tip, reducing prototyping costs through simulations,
- Implementing the most favourable simulation's nozzle and structure resulted in an immediate reduction in temperature, an increased lifespan of components, and decreased machine downtime, with a 4.49% increase in equipment availability and
- While initial economic gains remain uncertain, the current nozzle has outperformed its predecessor, successfully addressing the initial problem and meeting all requirements.

## 6. Future Considerations

Despite the significant value the developed work has shown for the institution, the development and innovation process cannot remain stagnant. Hence, this subsection will enumerate some improvements to the hot-chamber Zamak alloy injection process.

- Develop a new concept for the lower structure to facilitate the removal of the mould and extractors without requiring complete removal. This will keep the nozzle engaged and reduce the likelihood of damage.
- Implement thermal insulation for the crucibles and tip resistances to reduce energy loss from heat dissipation to the surrounding environment.

## Author Contributions

R.D.S.G.C., P.L.: conceptualization; A.F.V.P., P.L., R.d.C.M.S.-C., R.R.L.: methodology; A.F.V.P., P.L.: data curation; A.F.V.P., R.d.C.M.S.-C., P.L., R.R.L.: writing—original draft preparation; P.L.: investigation; R.D.S.G.C., A.G.P.: supervision; R.D.S.G.C., C.R.R.: validation; A.G.P., C.R.R.: visualization; A.F.V.P., R.d.C.M.S.-C., R.R.L.: writing—reviewing and editing. All authors have read and agreed to the published version of the manuscript.

## Acknowledgements

The authors thank the Polytechnic Institute of Porto—Instituto Superior de Engenharia do Porto—IPP/ISEP for the infrastructure offered for the development of this project and Centro Paula Souza—College of Technology São José dos Campos, Professor Jessen Vidal, FATEC/SJC- Brazil, for supporting the internationalisation of the RJJ project in partnership with IPP-ISEP-Porto, Portugal.

## Funding

The work is developed under the “DRIVOLUTION—Transition to the factory of the future”, with the reference DRIVOLUTION C644913740-0000022 research project, supported by European Structural and Investment Funds with the “Portugal2020” program scope.

## Institutional Review Board Statement

Not applicable.

## Informed Consent Statement

Not applicable.

## Data Availability Statement

Not applicable.

## Conflicts of Interest

The authors declare no conflict of interest.

## References

1. Williamson, R. Exchange rate exposure and competition: Evidence from the automotive industry. *J. Financ. Econ.* **2001**, *59*, 441–475. [https://doi.org/10.1016/S0304-405X\(00\)00093-3](https://doi.org/10.1016/S0304-405X(00)00093-3).
2. Pichler, M.; Krenmayr, N.; Schneider, E.; et al. EU industrial policy: Between modernisation and transformation of the automotive industry. *Environ. Innov. Soc. Transit.* **2021**, *38*, 140–152. <https://doi.org/10.1016/j.eist.2020.12.002>.
3. Costa, R.J.S.; Silva, F.J.G.; Campilho, R.D.S.G. A novel concept of agile assembly machine for sets applied in the automotive industry. *Int. J. Adv. Manuf. Technol.* **2017**, *91*, 4043–4054. <https://doi.org/10.1007/s00170-017-0109-4>.
4. Oduguwa, P.A.; Roy, R.; Sackett, P.J. Cost impact analysis of requirement changes in the automotive industry: A case study. *Proc. Inst. Mech. Eng. Part B J. Eng. Manuf.* **2006**, *220*, 1509–1525. <https://doi.org/10.1243/09544054JEM275>.
5. Kabak, O.; Ülengin, F.; Önsel, S.; et al. Cumulative belief degrees approach for analysing the competitiveness of the automotive industry. *Knowl. Based Syst.* **2014**, *70*, 15–25. <https://doi.org/10.1016/j.knosys.2013.09.006>.
6. Sarkar, M.; Park, K.S. Reduction of makespan through flexible production and remanufacturing to maintain the multi-stage automated complex production system. *Comput. Ind. Eng.* **2023**, *177*, 108993. <https://doi.org/10.1016/j.cie.2023.108993>.
7. Costa, M.J.R.; Gouveia, R.M.; Silva, F.J.G.; et al. How to solve quality problems by advanced fully-automated manufacturing systems. *Int. J. Adv. Manuf. Technol.* **2018**, *94*, 3041–3063. <https://doi.org/10.1007/s00170-017-0158-8>.
8. Rosa, C.; Silva, F.J.G.; Ferreira, L.P. Improving the quality and productivity of steel wire-rope assembly lines for the automotive industry. *Procedia Manuf.* **2017**, *11*, 1035–1042. <https://doi.org/10.1016/j.promfg.2017.07.214>.
9. Moreira, B.M.D.N.; Gouveia, R.M.; Silva, F.J.G.; et al. A novel concept of production and assembly processes integration. *Procedia Manuf.* **2017**, *11*, 1385–1395. <https://doi.org/10.1016/j.promfg.2017.07.268>.
10. Zhang, X.; Ming, X.; Bao, Y. A flexible smart manufacturing system in mass personalisation manufacturing model based on multi-module-platform, multi-virtual-unit, and multi-production-line. *Comput. Ind. Eng.* **2022**, *171*, 108379. <https://doi.org/10.1016/j.cie.2022.108379>.

11. Pekaric, I.; Sauerwein, C.; Haselwanter, S.; et al. A taxonomy of attack mechanisms in the automotive domain. *Comp. Stand. Interf.* **2021**, *78*, 103539. <https://doi.org/10.1016/j.csi.2021.103539>.
12. Van Straten, B.; Tantuo, B.; Dankelman, J.; et al. eprocessing Zamak laryngoscope blades into new instrument parts; an ‘all-in-one’ experimental study. *Heliyon* **2022**, *8*, e11711. <https://doi.org/10.1016/j.heliyon.2022.e11711>.
13. Wang, J.; Meng, B.; Zhang, L.; et al. Degradation modeling and reliability estimation for mechanical transmission mechanism considering the clearance between kinematic pairs. *Reliab. Eng. Syst. Saf.* **2024**, *247*, 110093. <https://doi.org/10.1016/j.ress.2024.110093>.
14. Eiras, E.; Silva, F.J.G.; Campilho, R.D.S.G.; et al. A Novel Fully Automatic Concept to Produce First Subset of Bowden Cables, Improving Productivity, Flexibility, and Safety. *Machines* **2023**, *11*, 992. <https://doi.org/10.3390/machines11110992>.
15. Du, H.; Jiang, Q.; Xiong, W. Computer-assisted assembly process planning for the installation of flexible cables modeled according to a viscoelastic Cosserat rod model. *Proc. Inst. Mech. Eng. Part B J. Eng. Manuf.* **2023**, *237*, 1737–1747. <https://doi.org/10.1177/09544054221136000>.
16. Vieira, D.; Silva, F.J.G.; Campilho, R.D.S.G.; et al. Automating Equipment towards Industry 4.0: A New Concept for a Transfer System of Lengthy and Low-Stiffness Products for Automobiles. *J. Test. Eval.* **2022**, *50*, 2310–2325. <https://doi.org/10.1520/JTE20210721>.
17. Treiber, W.G., Jr. Enhanced product design with hot-chamber magnesium die casting. *Mats. Des.* **1987**, *8*, 350–353. <https://doi.org/10.1016/j.matpr.2020.11.346>.
18. Li, T.; Song, J.; Zhang, A.; et al. Progress and prospects in Mg-alloy super-sized high pressure die casting for automotive structural components. *J. Mg Alloys* **2023**, *11*, 4166–4180. <https://doi.org/10.1016/j.jma.2023.11.003>.
19. Fu, M.W.; Zheng, J.-Y. Die Casting for Fabrication of Metallic Components and Structures. *Encyc. Mat. Metals Alloys* **2022**, *4*, 54–72. <https://doi.org/10.1016/B978-0-12-819726-4.00037-5>.
20. Wang, H.; Djambazov, G.; Pericleous, K.A.; et al. Modelling the dynamics of the tilt-casting process and the effect of the mould design on the casting quality. *Comp. Fluids* **2010**, *42*, 92–101. <https://doi.org/10.1016/j.compfluid.2010.11.010>.
21. Pereira, J.L.T.A.; Campilho, R.D.S.G.; Silva, F.J.G.; et al. Improving the Efficiency of the Bowden Cable Terminal Injection Process for the Automotive Industry. *Processes* **2022**, *10*, 1953. <https://doi.org/10.3390/pr10101953>.
22. Pinto, H.; Silva, F.J.G. Optimisation of Die Casting Process in Zamak Alloys. *Procedia Manuf.* **2017**, *11*, 517–525. <https://doi.org/10.1016/j.promfg.2017.07.145>.
23. Silva, F.J.G.; Campilho, R.D.S.G.; Ferreira, L.P.; et al. Establishing Guidelines to Improve the High-Pressure Die Casting Process of Complex Aesthetics Parts. *Transdiscipl. Eng. Methods Soc. Innov. Ind.* **2018**, *7*, 887–896. <https://doi.org/10.3233/978-1-61499-898-3-887>.
24. Pinto, H.A.; Silva, F.J.G.; Martinho, R.P.; et al. Improvement and validation of Zamak die casting moulds. *Procedia Manuf.* **2019**, *38*, 1547–1557. <https://doi.org/10.1016/j.promfg.2020.01.131>.
25. Sousa, V.F.C.; Silva, F.J.G.; Campilho, R.D.S.G.; et al. Developing a Novel Fully Automated Concept to Produce Bowden Cables for the Automotive Industry. *Machines* **2022**, *10*, 290. <https://doi.org/10.3390/machines10050290>.
26. Olbrich, S.; Lackinger, J. Manufacturing Processes of automotive high-voltage wire harnesses: State of the art, current challenges and fields of action to reach a higher level of automation. *Procedia CIRP* **2022**, *107*, 653–660. <https://doi.org/10.1016/j.procir.2022.05.041>.
27. Peffers, K.; Tuunanen, T.; Rothenberger, M.A.; et al. Positioning and presenting design science research for maximum impact. *J. Manag. Inf. Syst.* **2007**, *24*, 45–77. <https://doi.org/10.25300/MISQ/2013/37.2.01>.
28. Hevner, A.; Gregor, S. Envisioning entrepreneurship and digital innovation through a design science research lens: A matrix approach. *Inf. Manag.* **2022**, *59*, 103350. <https://doi.org/10.1016/j.im.2020.103350>.
29. Abdullah, O.I.; Abbood, W.T.; Hussein, H.K. Development of automated liquid filling system based on the interactive design approach. *FME Trans.* **2020**, *48*, 838–945. <https://doi.org/10.5937/fme2004938A>.
30. Teixeira, J.G.; Patrício, L.; Huang, K.H.; et al. The MINDS Method: Integrating Management and Interaction Design Perspectives for Service Design. *J. Serv. Res.* **2017**, *20*, 240–258. <https://doi.org/10.1177/1094670516680033>.
31. Devitt, F.; Robbins, P. Design, Thinking and Science. In *Design Science: Perspectives from Europe*; Helfert, M., Donnellan, B., Eds.; Springer: Cham, Switzerland, 2013. ISBN: 978-3-319-04089-9.
32. Siedhoff, S. Design science research. In *Seizing Business Model Patterns for Disruptive Innovations*; Springer: Cham, Switzerland, 2019; pp. 29–43. ISBN 978-3658263355; ISBN: 978-3-658-26336-2.
33. Lepeniotti, K.; Bousdekis, A.; Apostolou, D.; et al. Prescriptive analytics: Literature review and research challenges. *Int. J. Inf. Manag.* **2020**, *50*, 57–70. <https://doi.org/10.1016/j.ijinfomgt.2019.04.003>.
34. Tojal, M.C.; Silva, F.J.G.; Campilho, R.D.S.G.; et al. Case-based product development of a high-pressure die casting injection subset using design science research. *FME Trans.* **2022**, *50*, 32–45. <https://doi.org/10.5937/fme2201032T>.

35. Zhou, Z.; Tang, J.; Ding, H. Accurate modification methodology of universal machine tool settings for spiral bevel and hypoid gears. *Proc. Inst. Mech. Eng. Part B J. Eng. Manuf.* **2018**, 232, 339–349. <https://doi.org/10.1177/0954405416640173>.
36. Rosochowska, R.B.M. Measurements of thermal contact conductance. *J. Mat. Proc. Techn.* **2003**, 135, 204–210. [https://doi.org/10.1016/S0924-0136\(02\)00897-X](https://doi.org/10.1016/S0924-0136(02)00897-X).
37. Burte, P.R.; Im, Y.-T.; Altan, T.; et al. Measurement and analysis of heat transfer and friction during hot forging. *J. Manuf. Sci. Eng.* **1990**, 112, 332–339. <https://doi.org/10.1115/1.2899596>.
38. Marcolin, P.; Longhi, M.; Zini, L.P.; et al. Effects of the Casting Temperature in the Leakage of Zamak 5. *Mat. Sci. Forum* **2017**, 899, 458–462. <https://doi.org/10.4028/WWW.SCIENTIFIC.NET/MSF.899.458>.
39. Salman, A.S.; Abdulrazzaq, N.M.; Oudah, S.K.; et al. Experimental investigation of the impact of geometrical surface modification on spray cooling heat transfer performance in the non-boiling regime. *Int. J. Heat Mass Transf.* **2019**, 133, 330–340, <https://doi.org/10.1016/J.IJHEATMASSTRANSFER.2018.12.058>.
40. Chen, J. Injection Nozzle with Enhanced Heat Transfer Characteristics. U.S. Patent 8,475,157, 2 July 2013.
41. Saifullah, A.B.M.; Masood, S.H.; Sbarski, I. Thermal-structural finite element analysis of injection moulding dies with optimized cooling channels. *Sci. Forum* **2010**, 654–656, 1646–1649, <https://doi.org/10.4028/WWW.SCIENTIFIC.NET/MSF.654-656.1646>.